

## *Chapter - 5*

**To study the effect of active compound and active fractions of *Bauhinia variegata* L. on cell migration & cell death parameters in lung cancer cell lines (A549 and H460).**

## **5.1 Introduction**

Cell migration is a key factor in the metastatic spread of lung cancer cells to other parts of the body. This process is tightly regulated and is responsible for events, such as embryonic development, wound healing, and cancer metastasis<sup>1</sup>. Cells migrate through complex microenvironments by reacting to various extracellular signals<sup>2</sup>. The migration of cells is enabled by several interconnected cellular mechanisms, including adhesion, cytoskeletal rearrangement, and different signalling pathways<sup>3</sup>. Aberrant cell migration can lead to the development of cancer metastasis, which is the primary cause of lung cancer-related deaths<sup>4,5,6</sup>.

Lung cancer cells can be induced to undergo cell death by various internal and external stimuli, such as DNA damage, oxidative stress, and infection<sup>7</sup>. Different types of cell death mechanisms have been identified and studied extensively in the context of lung cancer, including Apoptosis, Necrosis, and Autophagy. Apoptosis is a process of programmed cell death that plays a crucial role in regulating cell growth and eliminating abnormal cells<sup>8,9</sup>. However, it is often dysregulated in cancer, including lung cancer<sup>10</sup>. Caspases, a group of proteases, are central to the apoptotic process, activating downstream substrates through cleavage<sup>11</sup>. The dysregulation of apoptosis is a significant contributor to the development and progression of lung cancer. Thus, targeting caspases has emerged as a potential therapeutic approach, with various caspase inhibitors currently in development and testing in preclinical and clinical studies<sup>12</sup>. The regulation of cell death is crucial for the prevention and treatment of lung cancer.

Various methods have been developed to investigate cell death parameters in lung cancer, including DAPI staining, Comet assay, ROS detection, MDC staining, and TMRM staining. DAPI staining is a technique that can be used to visualize changes in nuclear morphology in lung cancer cells<sup>13,14</sup>. The comet assay is another widely used technique that can be used to detect DNA damage in lung cancer cells<sup>15,16</sup>. ROS detection can be used to measure the levels of reactive oxygen species (ROS) in lung cancer cells, which play an important role in cancer development and progression<sup>17,18,19,20</sup>. MDC (Monodansylcadaverine) staining is a technique that can be used to detect the accumulation of autophagic vacuoles in lung cancer cells<sup>21,22</sup>. TMRM (Tetramethyl rhodamine) staining can be used to measure mitochondrial membrane potential, which is an essential parameter for mitochondrial function and cellular energy production in lung cancer cells<sup>22,23</sup>. Understanding the molecular mechanisms underlying cell migration and cell death in lung cancer is crucial for the development of new therapeutic strategies.

## **5.2 Material and methods**

### **5.2.1 Chemicals**

Cell culture experimental design same as mentioned in material and methods (chapter 4), Normal agarose was obtained from Himedia, low gelling temperature agarose was purchased from Sigma-Aldrich, Disodium ethylene diamine tetra acetic acid (Na<sub>2</sub>EDTA) from SRL, Tris-base, EDTA, Crystal violet and Trypan blue dye from Himedia, Ammonium per-sulphate, Sodium lauryl sarcosinate was obtained from Sigma-Aldrich, Glycine was obtained from Himedia, Sodium- dodecyl sulphate was obtained from Himedia, Acrylamide and Bis-acrylamide were obtained from Sigma-Aldrich.

### **5.2.2 Scratch assay/ Wound healing assay**

**Principle-** During metastasis, cancer cells go through an epithelial to mesenchymal transition. Cancer cells separate and migrate as a result of a loss in adhesion. The fundamental procedures include making a "scratch" in a cell monolayer, taking pictures after staining at the start and at predetermined intervals. The distance the cells have moved will be shown by comparing the photos.

#### **Protocol:**

A549 and H460 cells were grown & maintained (as discussed in section 3.7). Further, A549 cells were treated with different concentrations of **Oleic acid for 48 h (as mentioned in section 4.5.1.2.4, chapter 4) and H460 cells with different concentrations of PFF3 and PFF4 (as mentioned in section 4.5.2.2, chapter 4) and also with combination concentration of PXT and PFF3 for 24 h (as mentioned in section 4.6.2.1, chapter 4)**. Paclitaxel was used as a positive control. Concentrations of Paclitaxel on A549 was defined based on the literature study<sup>24</sup>. Plates were placed in an incubator at 37 °C for 0-36h depending upon the cells. A549 and H460 cells were stained with crystal violet and images were captured at different time-points from 0 to 36 h respectively. The pictures acquired for every sample was further analyzed quantitatively by using computing software (Image J).

### **5.2.3 Analysis of Intracellular Reactive Oxygen Species by DCHF-DA**

**Principle:** DCFDA assay involves adding a non-fluorescent dye called DCHF-DA to cancer cells, which is converted into DCFH by esterases within the cells. DCFH is then oxidized by ROS, resulting in the production of a highly fluorescent compound called DCF. The amount

## **Effect of phytocomponents from *Bauhinia variegata* L. on Lung cancer cell lines**

of DCF fluorescence is proportional to the amount of ROS present within the cells. Therefore, measuring DCF fluorescence intensity enables to quantify ROS levels in cancer cells and provide information about the role of ROS in cancer development and drug efficacy.

### **Protocol:**

A549 cells were treated with different concentrations of **Oleic acid for 48 h and H460 cells with different concentrations of PFF3 and PFF4 and also with combination concentration of PXT and PFF3 for 24 h**. Paclitaxel was used as a positive control. At the end of the incubation period, the media was removed and 10  $\mu$ M of DCHF-DA<sup>22</sup> which is diluted in media was added to the cells and incubated for 30 min at 37 °C. The cells were then washed thrice with PBS and images were taken by fluorescence microscope (Olympus, USA).

### **5.2.4 Fluorescent Microscopy Analysis by**

#### **5.2.4.1 DAPI Staining**

#### **5.2.4.2 Acridine Orange/Ethidium Bromide Staining**

#### **5.2.4.3 Annexin V and PI staining**

**Principle:** DAPI binds to the minor groove of double-stranded DNA and stains the nucleus of the cells. The fundamental concept of using acridine orange and ethidium bromide dyes in cancer cell research is based on their ability to attach to nucleic acids within cells and produce distinctive fluorescence signals that are indicative of the DNA's integrity. It differentiate between cells at varying stages of apoptosis. Annexin V detects apoptosis by binding to exposed phosphatidylserine on the outer surface of the plasma membrane, while PI detects necrosis by binding to DNA in cells with a damaged membrane by fluorescence microscopy.

### **Protocol:**

Cell nuclear morphology was checked by fluorescence microscopy using **DAPI<sup>22,25</sup>** and **AO/EtBr<sup>26</sup>** staining. A549 cells were treated with the different concentrations of **Oleic acid for 48 h** and H460 cells with **different concentrations of PFF3 and PFF4 and also with combination concentration of PXT and PFF3 (H460) for 24 h** followed by DAPI (5mg/ml) and AO/EB dye (100 $\mu$ g/ml AO and 100 $\mu$ g/ml EtBr) mix and examined under a Nikon Eclipse Ti fluorescence microscope. For Annexin V and PI staining, after respective treatment on H460

## **Effect of phytocomponents from *Bauhinia variegata* L. on Lung cancer cell lines**

cell line, cells were rinsed with 0.01 M PBS and suspended in 200 $\mu$ L binding buffer. After that, cells were incubated for 30 minutes at 4 °C in a dark environment with 10  $\mu$ L Annexin V-FITC, and 5  $\mu$ L PI. Annexin V-FITC and PI fluorescence was immediately observed under fluorescence microscope (Olympus, Tokyo, Japan).

### **5.2.5 Comet assay- DNA damage by Single gel electrophoresis**

Qualitative DNA damage was assessed by comet assay (Single cell gel electrophoresis) according to the protocol of Olive *et al.* (2006)<sup>27</sup>.

**Principle:** The comet assay, also known as single-cell gel electrophoresis assay, is a technique used to measure DNA damage in individual cells. The principle behind the assay is that DNA damage caused by factors like radiation or chemicals can lead to the formation of a comet-like tail during electrophoresis. In cancer cells, DNA damage can occur due to various reasons. Therefore, the comet assay can be used to detect and quantify DNA damage in cancer cells, helping researchers better understand carcinogenesis and develop new cancer therapies.

#### **Protocol:**

1. Normal agarose (1%): One gram of normal melting point agarose was dissolved in 100ml of double distilled water.
2. Low-melting point agarose (LMPA) (1%): One gram of low melting point agarose was dissolved in 100ml of double distilled water.
3. Sample preparation: 1% molten agarose is used to prepare agarose-precoated slides by immersing them in it and wiping one side clean. Let the agarose air-dry to a thin layer. Slides may be prepared beforehand. To coated plates, add 75 $\mu$ L LMPA mixed with 10,000 cells. Using hemocytometer, adjust the cell number.
5. **Alkaline Lysis and Electrophoresis:** Slides should be placed in a covered dish containing A1 lysis solution (1.2M NaCl, 100mM Na<sub>2</sub>EDTA, 0.1% sodium lauryl Sarcosinate, 0.26 M NaOH (pH>13) after the agarose has gelled. Do not pour solutions over slides or shake containers containing slides; instead, gently handle the slides by holding them horizontally and lowering them into the solutions. Samples should be lysed at 4 °C in the dark for 18 to 20 hours. Slides should then be immersed in fresh A2 (alkaline rinse and lysis solution:0.03 M NaOH,

## **Effect of phytochemicals from *Bauhinia variegata* L. on Lung cancer cell lines**

2mM Na<sub>2</sub>EDTA, (pH – 12.3) solution in an electrophoresis chamber following these three rinses.

6. Run 25 minutes of electrophoresis in solution A2 at a 0.6 V/cm voltage and if utilizing 20 V, the current should be around 40 mA.

7. Slides should be removed from the electrophoresis chamber and rinsed in 400 ml of distilled water, and then neutralized. Slides should be stained for 20 minutes in a solution containing 2.5µg/ml of EtBr in a distilled water and incubate for 20 min.

8. Analyze each individual comet image using image J analysis tools to look for variables like overall intensity (DNA content), tail length, percent DNA in tail, and tail moment.

### **5.2.6 Mitochondrial Transmembrane Potential Assessment**

For analysing  $\Delta\psi_m$ , the control and treated cells medium was softly aspirated and 100µl of serum-free medium containing 50 nM TMRM dye (Molecular Probes, OR, USA) was added, as explained in the protocol<sup>28</sup>. Paclitaxel and Gemcitabine were used as a positive control. After 10 min incubation at 37 °C, images were captured using fluorescent microscope.

### **5.2.7 MDC (Monodansylcadaverine) staining**

**Principle:** MDC staining works by binding to the acidic vacuoles of autophagosomes and lysosomes in cells. As a basic dye, MDC accumulates in these structures and emits a bright green fluorescence upon excitation with blue light. Due to this property, MDC staining is frequently utilized to identify and measure autophagic activity within cells.

**Protocol:** A549 cells were grown in a 6-well plate, treated with different defined concentrations of OA for 48 h. Cells were then washed with cold-PBS, and incubated with 50µM MDC at 37°C for 30min. After washing, the stained cells were examined using a fluorescence microscope (Olympus, USA).

### **5.2.8 Western Blotting**

Cells were treated with different concentrations of OA for 48h. Cells were harvested, washed with ice cold PBS and lysed in NP40 Lysis buffer (150mM NaCl, 50mM Tris-Cl, 1% NP40, 1mM PMSF). Protein concentration was determined by Bradford assay and equal concentration of protein was loaded 12% SDS-PAGE. Protein was electroblotted on Nitrocellulose membrane at 105 V for 1 hour. Following the transfer, the membrane was blocked with 5%

## **Effect of phytocomponents from *Bauhinia variegata* L. on Lung cancer cell lines**

blocking buffer (5% non-fat dried milk and 0.1% tween-20 in TBS) for 1 hour at room temperature. The membrane was incubated overnight with specific primary antibody. After incubation the membrane was washed three times with TBS-T (TBS containing 0.1% Tween 20) for 10min and incubated with secondary antibody at room temperature for 1 hour. The membrane was again washed three times with TBS-T. Immunoreactive bands were visualized using ECL (enhanced chemiluminescence) reagents. Using the imaging J programme, the amount of each protein has been measured, and then a densitometric analysis of the ratio of the density of each target protein to the  $\beta$ -actin (for total protein) as described by <sup>23</sup>.

### **5.2.9 Statistical analysis**

All experiments were evaluated in triplicate (n = 3). Data are expressed as means  $\pm$  SEM. All statistical analyses were performed using GraphPad Prism 8.0 software. One-way and two-way ANOVA were used to analyse the sets of data. P value < 0.05 was considered statistically significant.

## **5.3 Results and discussion**

### **5.3.1 Scratch assay/ Wound healing assay**

#### **5.3.1.1 A549 cells treated with Oleic Acid showed slower migration**

Metastasis is one of the main outcomes seen in Non-small cell Lung cancer patients. Therefore, we have observed the effect of different concentrations of Oleic acid (OA) on this cellular property by scratch assay. Representative image (Figure 5.1 a) shows the wound diameter at different time points from 0 to 36 h after treatment with different concentrations of OA on A549 cells. In A549 cells, as compared with the control group, gradual reduction in migration was noticed within the number and rate of migrated cells with OA treatment. A slower rate of migration was observed with 100  $\mu$ M and 150  $\mu$ M treatment while at 200  $\mu$ M concentration, the cells were unable to survive. Hence, this dose was excluded from the study. In the Graph (Figure 5.1 b), the wound size at 150  $\mu$ M oleic acid is 220.7  $\mu$ m (for 30Hr) which is clearly indicating cell migration impairment (reduced wound size area) as compared with control at same concentration. A549 cells showed slower migration and wound healing at 150 $\mu$ M Oleic acid concentration as compared with control (not treated). OA showed greater inhibitory effect than Paclitaxel at defined concentrations. Thus, the Oleic acid found from Petroleum ether bark extract is able to impair the growth and migration of A549 cells at concentration range 150-200  $\mu$ M.

Effect of phytochemicals from *Bauhinia variegata* L. on Lung cancer cell lines

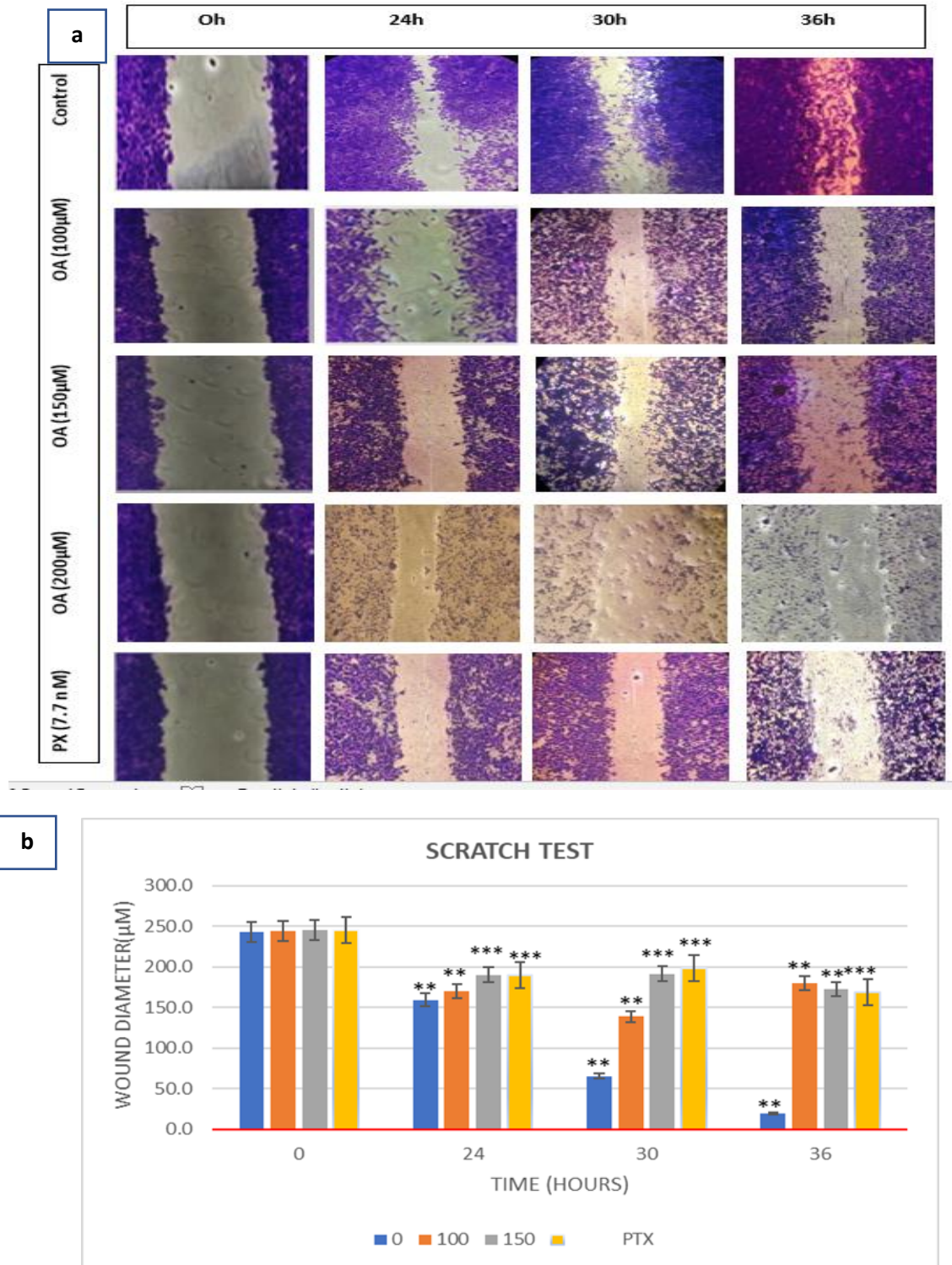
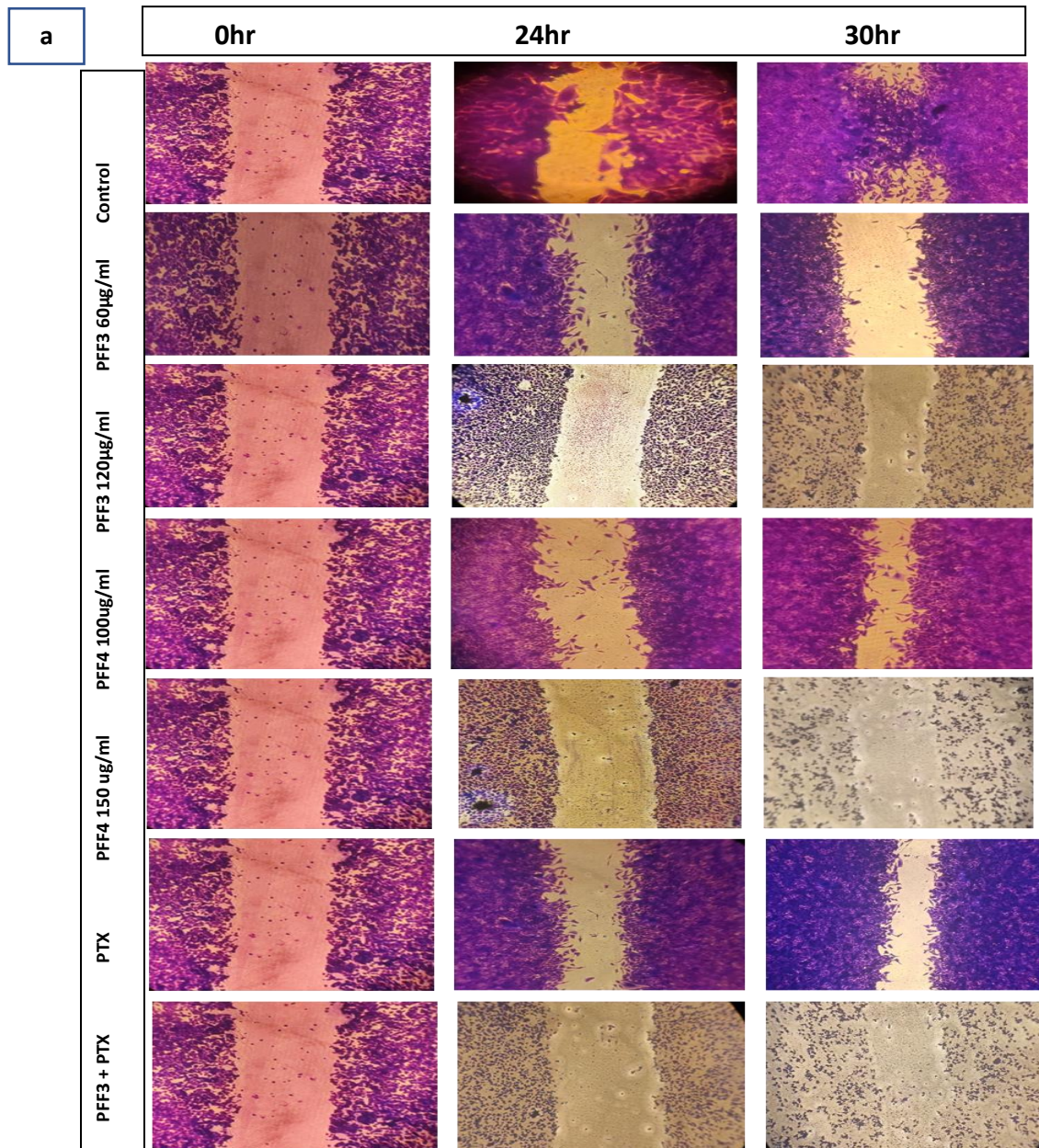


**Figure 5.1** *In vitro* scratch test to assess effect of OA on cell migration of A549 cells; n = 3. (a) Wound healing assay to determine the effect of OA on A549 cell migration at different concentrations for 36h. (b) Quantitative analysis of wound size ( $\mu\text{m}$ ) within 36 h. Error bars indicates the standard error of the mean of three independent experiments. \*\* $p < 0.01$ , \*\*\* $p < 0.001$ .

### 5.3.1.2 CBE fractions showed Slower Migration in H460 Treated cells

H460 cells showed slower migration and wound healing capacity with different concentrations of PFF3 and PFF4 as well as with PFF3 + Paclitaxel (PXT) treatment depending upon the dose and time respectively as shown in Figure 5.2 a. Cells showed slower migration and wound healing at 60µg/ml & 120µg/ml treatment for PFF3 and 100µg/ml & 150µg/ml treatment for PFF4 fractions at 24-30 hr time-points as compared to control. Migration of combination treatment of PFF3 (50µg/ml) & PXT (1.75nM) decreased significantly as compared with single agents after 24 hr and 30 hr treatments. In graph 5.2 b, the reduced wound size area is shown at different concentrations and time-points as compared to control.



## Effect of phytochemicals from *Bauhinia variegata* L. on Lung cancer cell lines

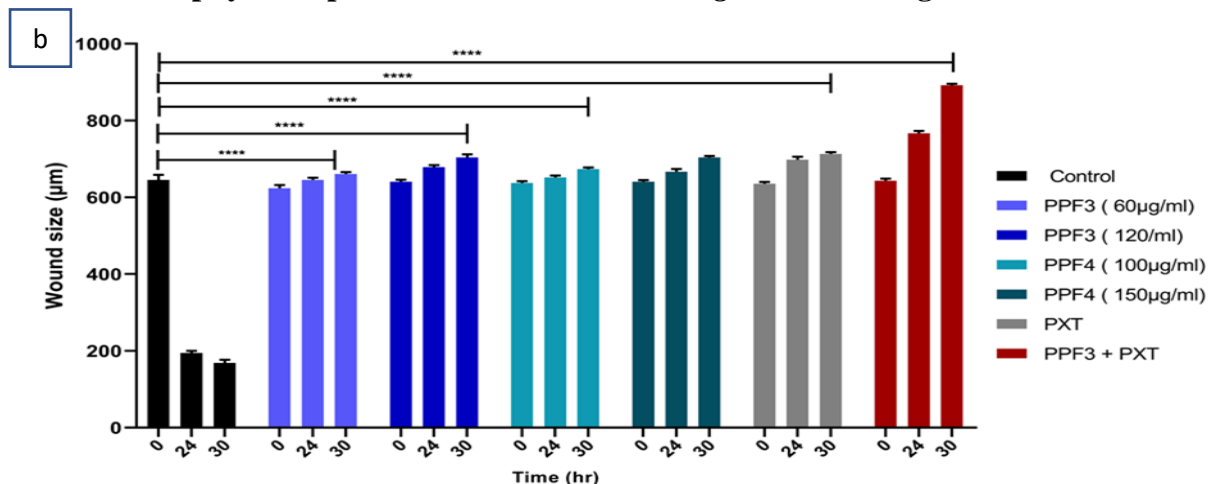
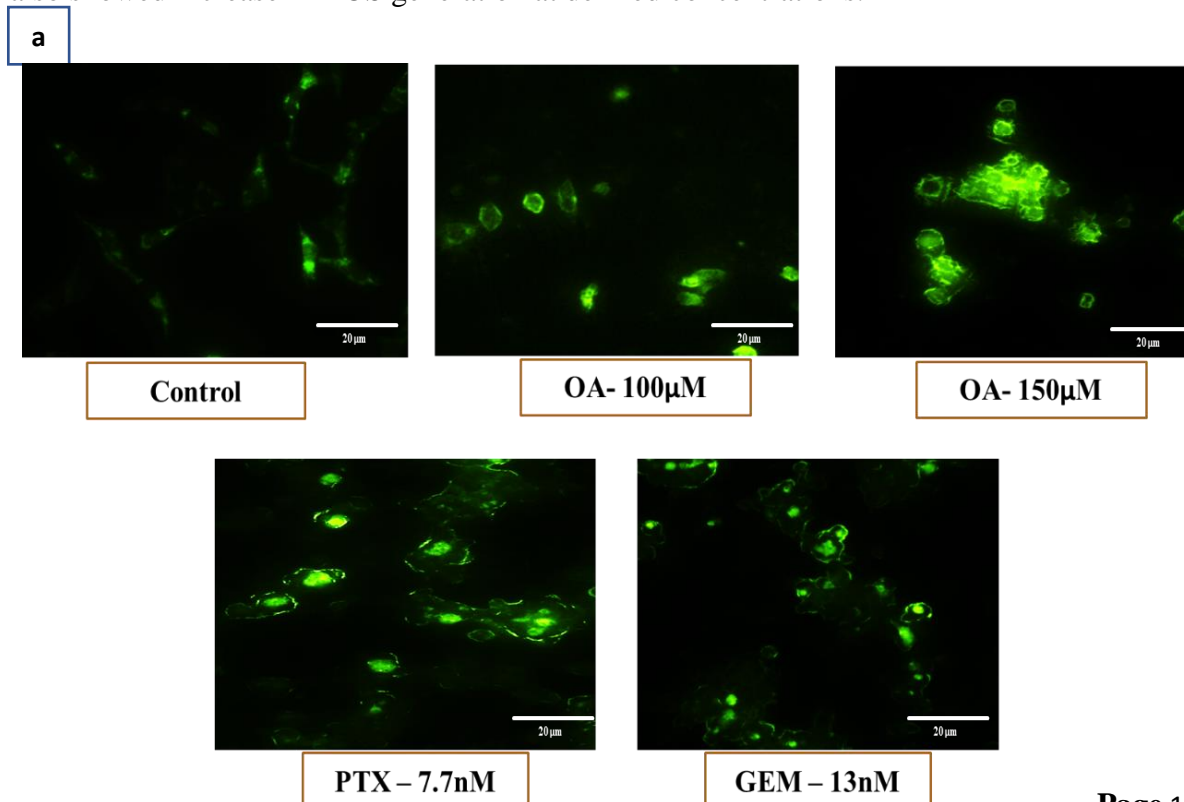


**Figure 5.2** *In vitro* scratch test to assess effect of PPF3, PPF4 and combination of PPF3 & PXT on cell migration of H460 cells (a) Wound healing assay to determine the effect of PPF3, PPF4 and combination of PPF3 & PXT on cell migration, at different concentrations for 30h. (b) Quantitative analysis of wound size ( $\mu\text{m}$ ) within 30 h. Error bars indicates the standard error of the mean of three independent experiments. \*\*\*\* $p < 0.0001$ .

### 5.3.2 Measurement of Intracellular ROS levels

#### 5.3.2.1 Effect of Oleic acid on Intracellular ROS levels of A549 cells

We used DCHF-DA as a molecular probe to detect intracellular ROS generation in A549 cells. After Oleic acid treatment with defined concentrations (as mentioned above) for 48 h, the ROS levels significantly increased in a concentration dependent manner, indicating Oleic acid promoted ROS generation in A549 cells as shown in Figure 5.3 a, b. PTX and Gemcitabine also showed increase in ROS generation at defined concentrations.



## Effect of phytochemicals from *Bauhinia variegata* L. on Lung cancer cell lines

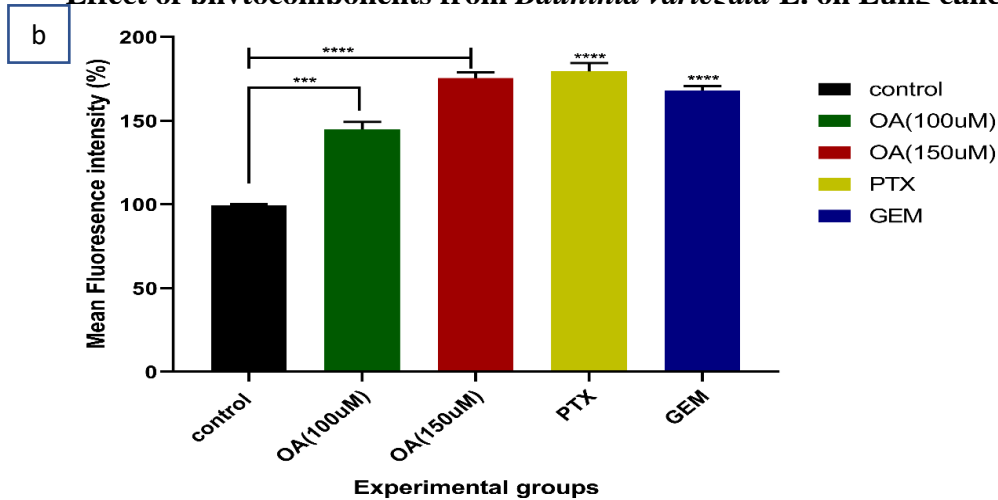
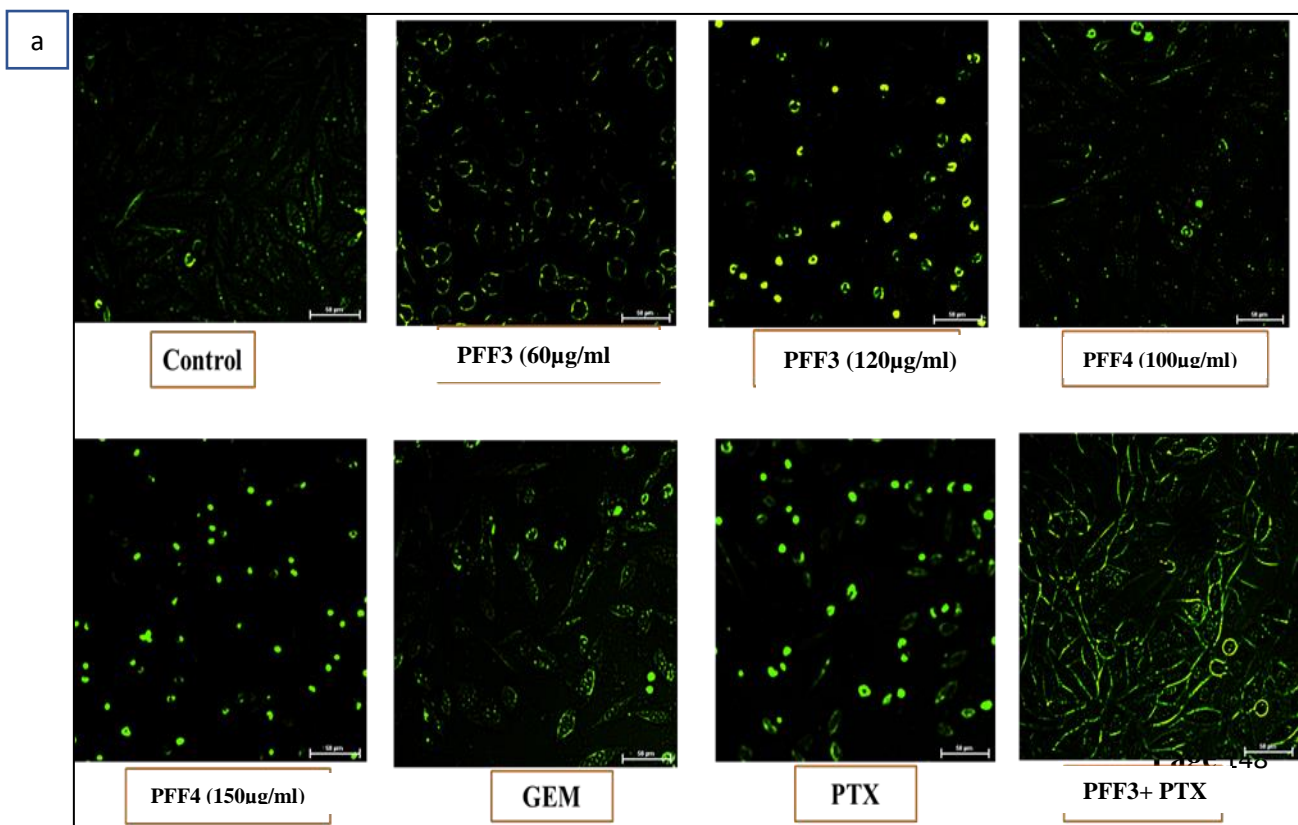


**Figure 5.3** Oleic acid promoted ROS generation in A549 cells in dose dependent manner. a) Fluorescence microscopy (x 400). b) Statistical analysis of fluorescence intensity was done by one-way ANOVA gives \*\*\* $p < 0.001$ , \*\*\*\* $p < 0.0001$ .

### 5.3.2.2 Effect of PFF3 & PFF4 on Intracellular ROS levels of H460 cells

H460 cells were treated with PFF3 and PFF4 with defined concentrations (as mentioned above) for 24 h and the ROS levels were found to be increasing significantly in a concentration dependent manner, means PFF3 and PFF4 promoted ROS generation in H460 cells as shown in Figure 5.4 a, b. Increased DCF values indicate rapidly generated intracellular ROS levels. ROS generation and the cell death caused by the combined therapy was also observed and it was found that the combination of PFF3 & PXT (50ug/ml +1.75nM) synergistically induced more ROS buildup in H460 cells than the single dose treatments as well as after PXT and Gemcitabine treatment as single agents shown in Figure 5.4.



## Effect of phytochemicals from *Bauhinia variegata* L. on Lung cancer cell lines

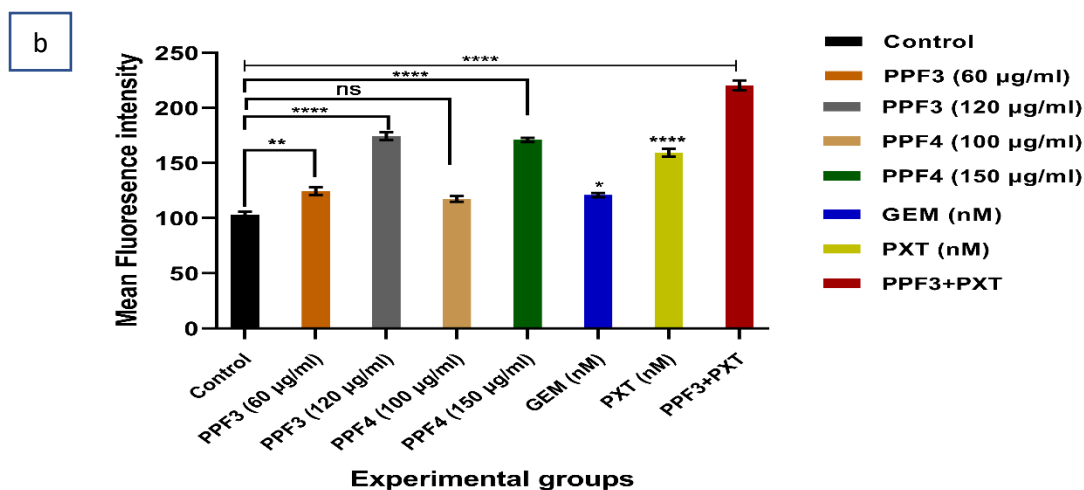
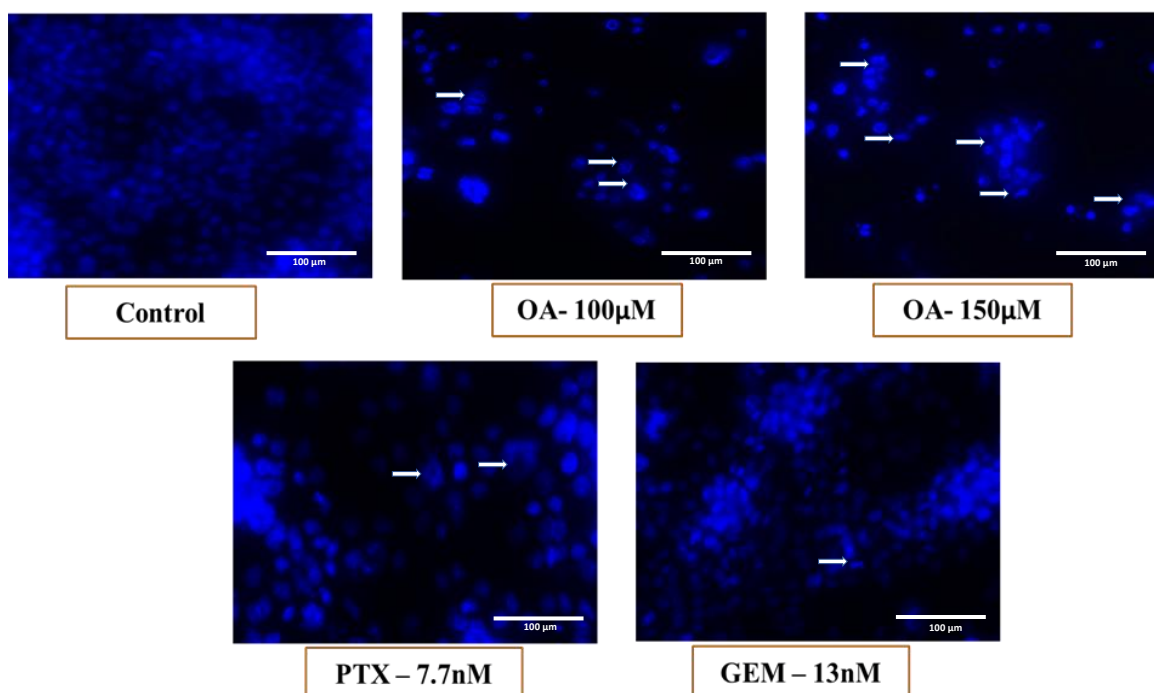


**Figure 5.4** PPF3 and PPF4 promoted ROS generation in H460 cells in dose dependent manner. PPF3 & PTX combination synergistically increased ROS production in H460 cells than as single agents. a) Fluorescence microscopy graph (x 400). b) Statistical analysis of fluorescence intensity was done by one-way ANOVA gives \*\*\* $p < 0.001$ , \*\*\*\* $p < 0.0001$ .

### 5.3.3 Fluorescent Microscopy Analysis by

#### 5.3.3.1 Study of cell morphology by DAPI staining (A549 cells)

Nuclear alterations that distinguish apoptosis from necrosis can be seen by DAPI staining. In the current work, A549 cells treated with the different concentrations of oleic acid for 48 hr showed alterations, indicative of apoptosis as shown in Figure 5.5 a. After treatment, A549 cells exhibit the morphological modifications linked to apoptosis, such as chromatin condensation, nuclear fragmentation, and nucleus margination as marked by arrows in figure 5.5a. Paclitaxel and Gemcitabine also show alterations which are indicative of apoptosis.



## Effect of phytocomponents from *Bauhinia variegata* L. on Lung cancer cell lines

**Figure 5.5** The effect of OA at different concentrations on apoptotic potential in A549 cells was evaluated using DAPI staining for 24 h under by fluorescence microscope (x 400). Arrow indicates chromatin condensation, nuclear fragmentation and cell shrinkage in treated cells as compared to control cells.

### 5.3.3.2 Study of cell morphology by DAPI staining (H460 cells)

H460 cells were treated with different concentrations of PFF3, PFF4 and combination of PFF3 and PTX for 24 hr. Depending upon the doses (as mentioned above), H460 cells exhibit morphological changes like chromatin condensation and nuclear fragmentations which are indicators of apoptosis. The combination of PFF3 & PXT (50ug/ml +1.75nM) synergistically induced more apoptosis in H460 cells than the single dose treatments as well as also after PXT and Gemcitabine treatment as single agents shown in Figure 5.6.

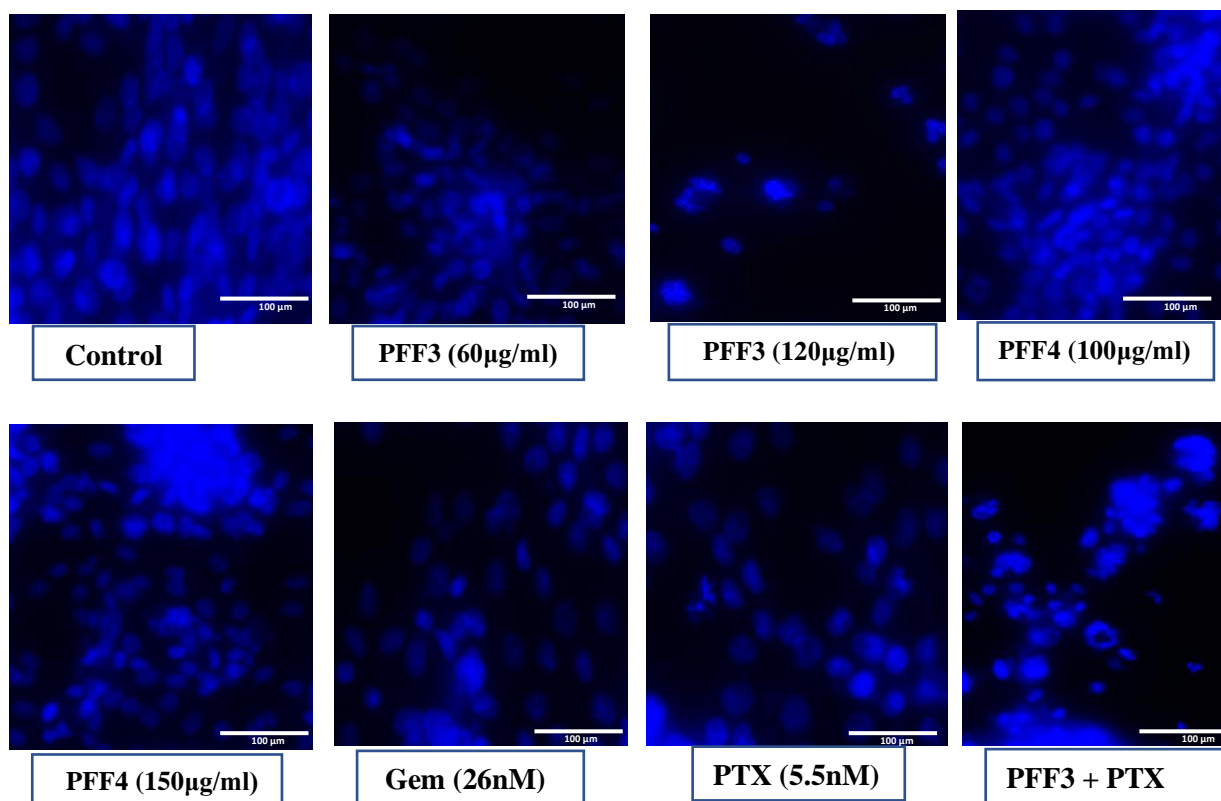


**Figure 5.6** The effect of PFF3, PFF4 and combination of PFF3 & PXT, at different concentrations on apoptotic potential in H460 cells was evaluated using DAPI staining for 24 h under by fluorescence microscope (x 400). Arrow indicates chromatin condensation, nuclear fragmentation and cell shrinkage in treated cells as compared to control cells.

### 5.3.3.3 Dual Acridine Orange (AO)/Ethidium Bromide (EtBr) Staining and Annexin V/ PI in H460 cells

#### 5.3.3.3.1 AO/EtBr staining (H460 cells)

## Effect of phytocomponents from *Bauhinia variegata* L. on Lung cancer cell lines

The H460 control group had a large number of live cells with normal morphology, but early apoptotic cells were seen after treatment with different concentrations of PFF3, PFF4 and combination of PFF3 & PXT (50 $\mu$ g/ml +1.75nM) for 24 hr. The treated group showed early-stage apoptotic cells, identified by yellow-green AO nuclear staining. Both early and late apoptotic cells were observed in H460 cells with increasing concentrations of PFF3 and PFF4. The IC50 treatment showed the greatest number of apoptotic bodies, and the cells were mostly in the late apoptotic stage as shown by arrows in Figure 5.7. Chromatin condensation and the development of apoptotic bodies are two signs that apoptosis had occurred, were seen in the nuclear alterations.

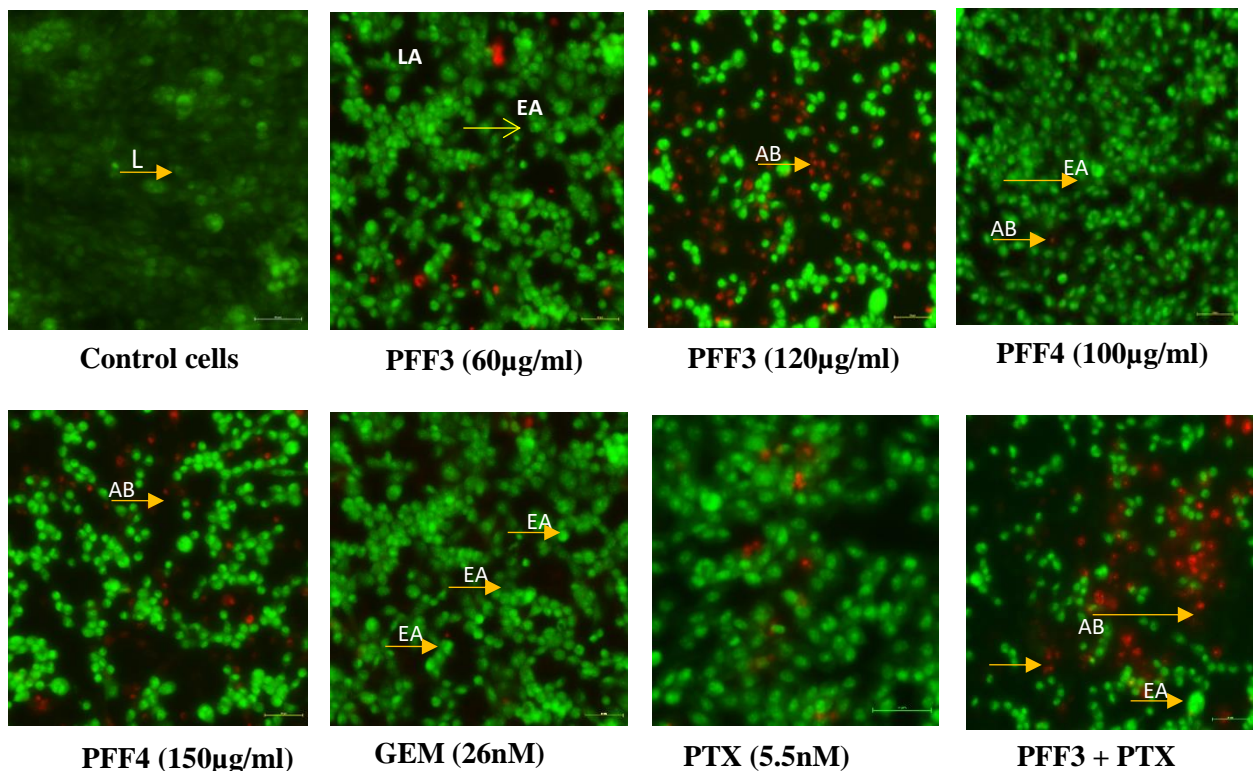


**Figure 5.7** H460 cells were stained by AO/EtBr and observed under fluorescence microscope (x 400). Green live cells showed normal morphology with uniform nuclei; yellow early apoptotic cells showed nuclear margination and chromatin condensation. Late orange/red apoptotic cells showed fragmented chromatin and apoptotic bodies.

### 5.3.3.3.2 Annexin V/ PI staining (H460 cells)

Annexin V-PI (Propidium iodide) staining is used to study cell apoptosis. Live cells with intact membranes appear unstained. Early apoptotic cells display Annexin V staining only, indicating phosphatidylserine translocation, while late apoptotic or necrotic cells show both Annexin V and PI staining, indicating membrane permeabilization. In vehicle control cells, annexin V-FITC and PI signals were barely detectable, but high fluorescence densities were evident in

## Effect of phytochemicals from *Bauhinia variegata* L. on Lung cancer cell lines

response to increasing concentrations of PFF3 and PFF4 on H460 cells as shown in Figure 5.8. The combination of PFF3 & PXT (50ug/ml +1.75nM) showed an increase in number of cells undergoing late apoptosis or necrosis, resulting in more cells showing Annexin V and PI staining. Cells treated with different concentrations of PFF4 showed more PI positive and reduced or less Annexin V stained cells, which reflects that they are in late apoptotic and necrotic stage. Cells showing yellow or orange staining pattern after treating with different concentrations of PFF3 and PFF4 in Annexin V-PI staining is an indication that cells are in the late stage of cell death.

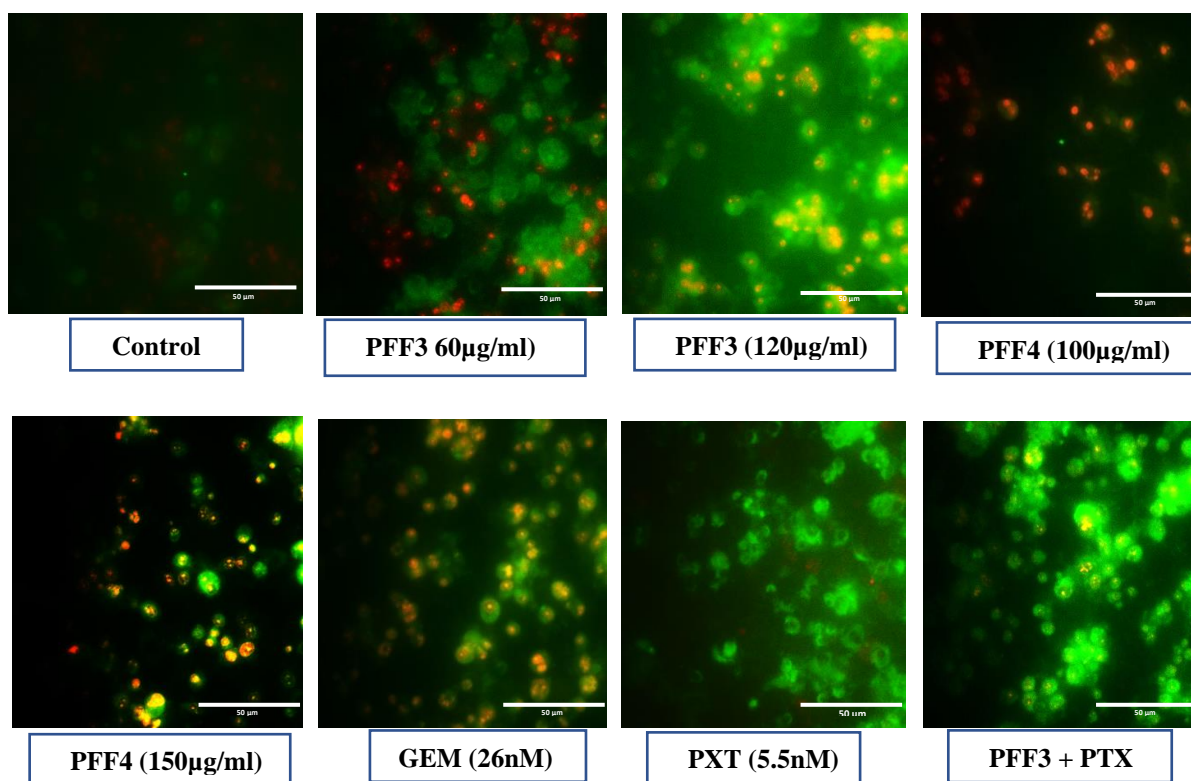


**Figure 5.8** Apoptosis detection on staining H460 cells with Annexin V and PI after treatment with different concentrations of PFF3 and PFF4 for 24 hr, by fluorescence microscopy.

### 5.3.4 Comet assay- DNA damage by Single gel electrophoresis

#### 5.3.4.1 *In vitro* DNA damage – In A549 cells

To comprehend the decline in overall cell viability in OA treated cells. Cells were treated with different concentrations of OA for 48 hours to see if DNA damage was induced. The DNA damage was then measured using a comet assay as shown in Figure 5.9. Paclitaxel (7.7 nM) and Gemcitabine (13nM) were used as positive controls and treated on A549 cells at defined concentrations. After visualizing under fluorescence microscope, comet like structures were

## Effect of phytocomponents from *Bauhinia variegata* L. on Lung cancer cell lines

seen in OA treated cells. The comet-like structures that form have a head and a tail. The head contains intact DNA that has not migrated towards the anode, while the tail indicates the amount of DNA damage. A longer tail corresponds to greater DNA damage in that cell. The findings showed that OA greatly increased DNA damage after 48 hours of treatment, causing comet tails to form in A549 cells.

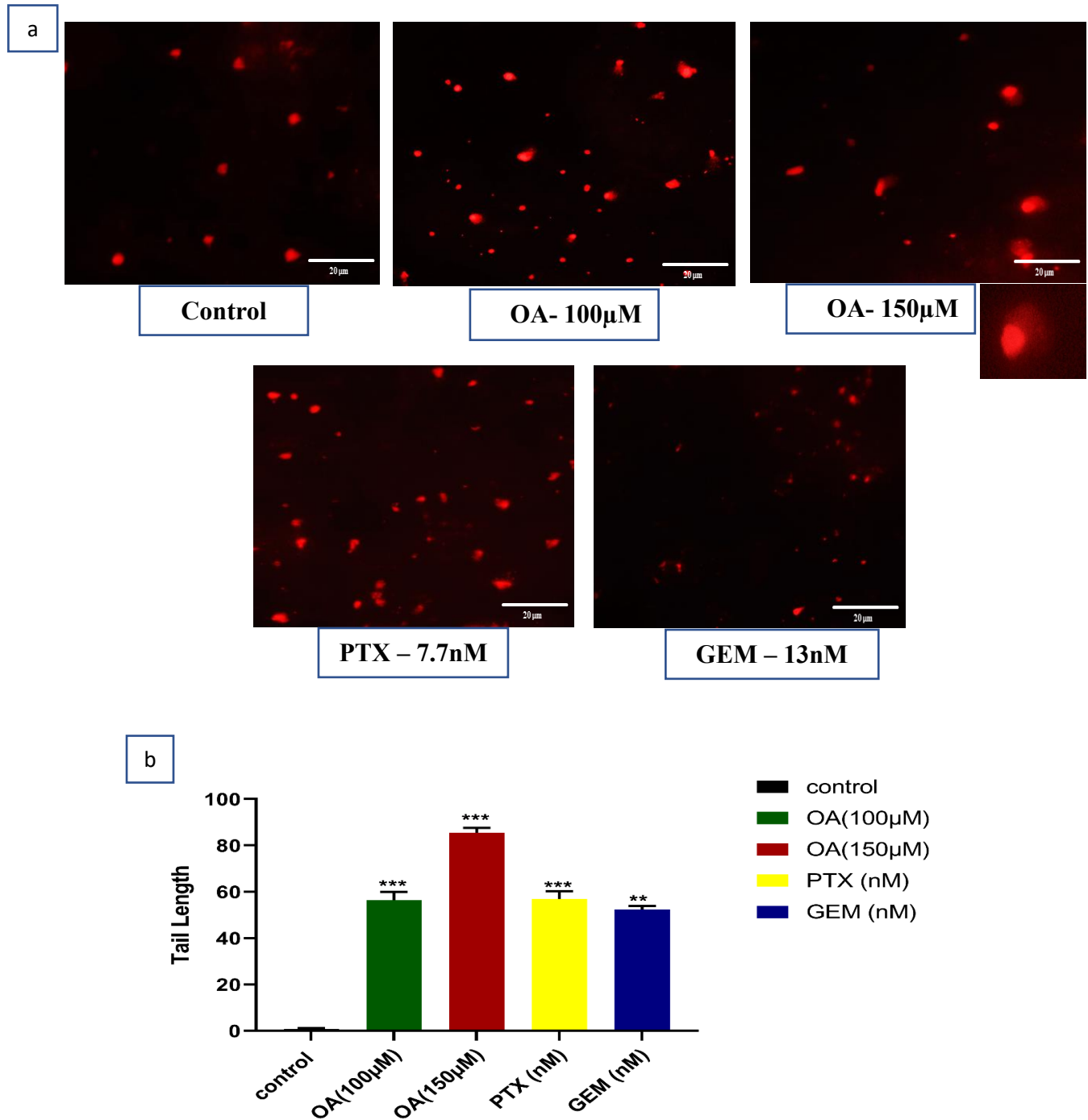
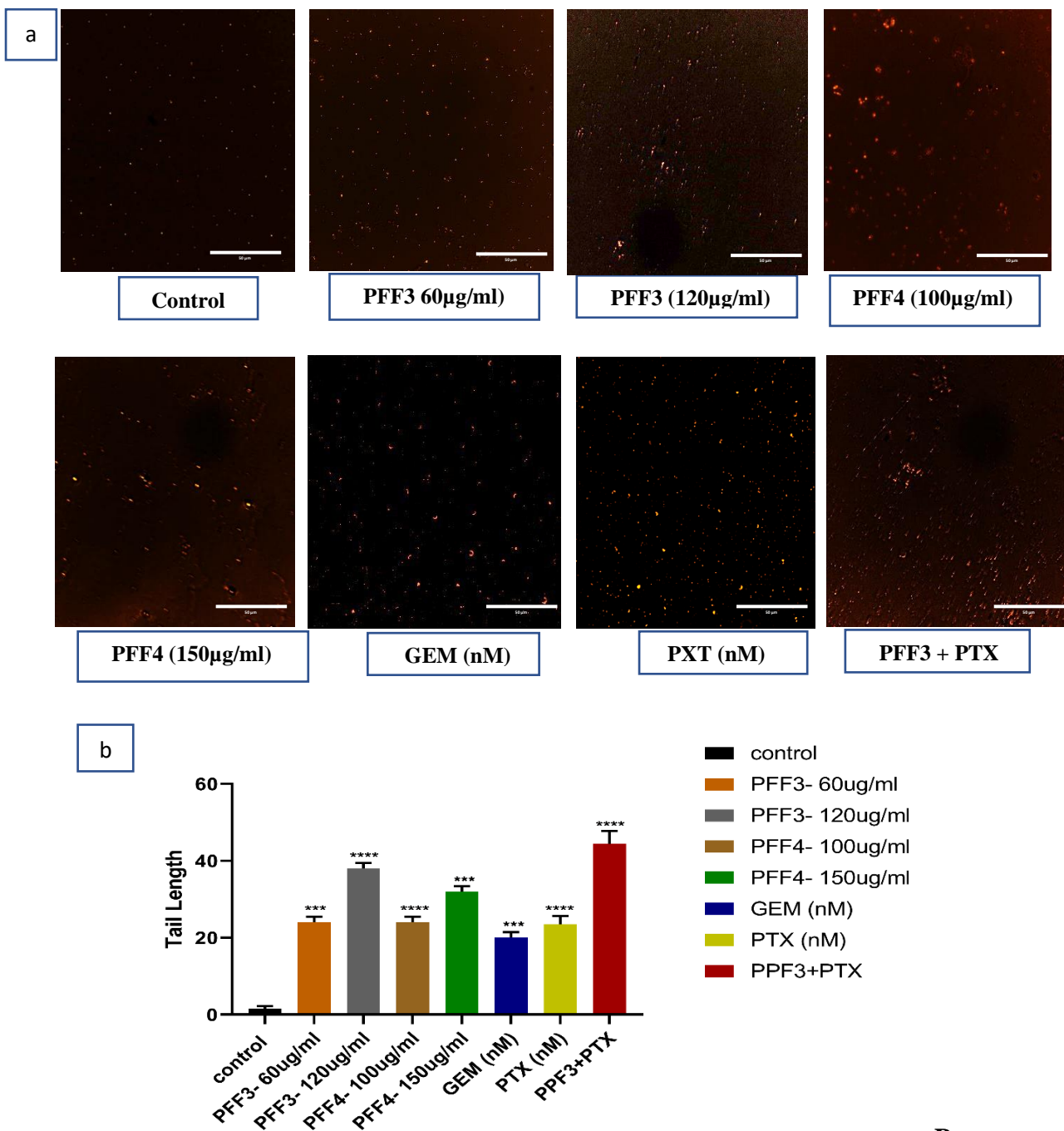


**Figure 5.9** Oleic acid induced DNA damage in A549 cells. (a) Cells were treated with different concentrations of OA for 48 hr and analyzed by comet assay. Enlarged comet of OA IC50. (b) Quantification of comet length (x 400).

## Effect of phytocomponents from *Bauhinia variegata* L. on Lung cancer cell lines

### 5.3.4.2 *In vitro* DNA damage – In H460 cells

H460 cells were treated with defined concentrations of PFF3 and PFF4 as well as with combination of PFF3 & PXT (50ug/ml +1.75nM) for 24 hours to see if DNA damage was induced. Figure 5.10 shows that the PFF3 and PFF4 higher concentrations promote DNA damage. The combination of PFF3 & PXT at (50ug/ml +1.75nM) showed maximum increase in DNA damage suggesting that it caused chromosomal DNA fragmentation, which resulted in apoptotic cell death. Thus, PFF3 and PFF4 higher concentrations as well as combination of PFF3 & PXT (50ug/ml +1.75nM) triggered DNA damage in H460 cells.



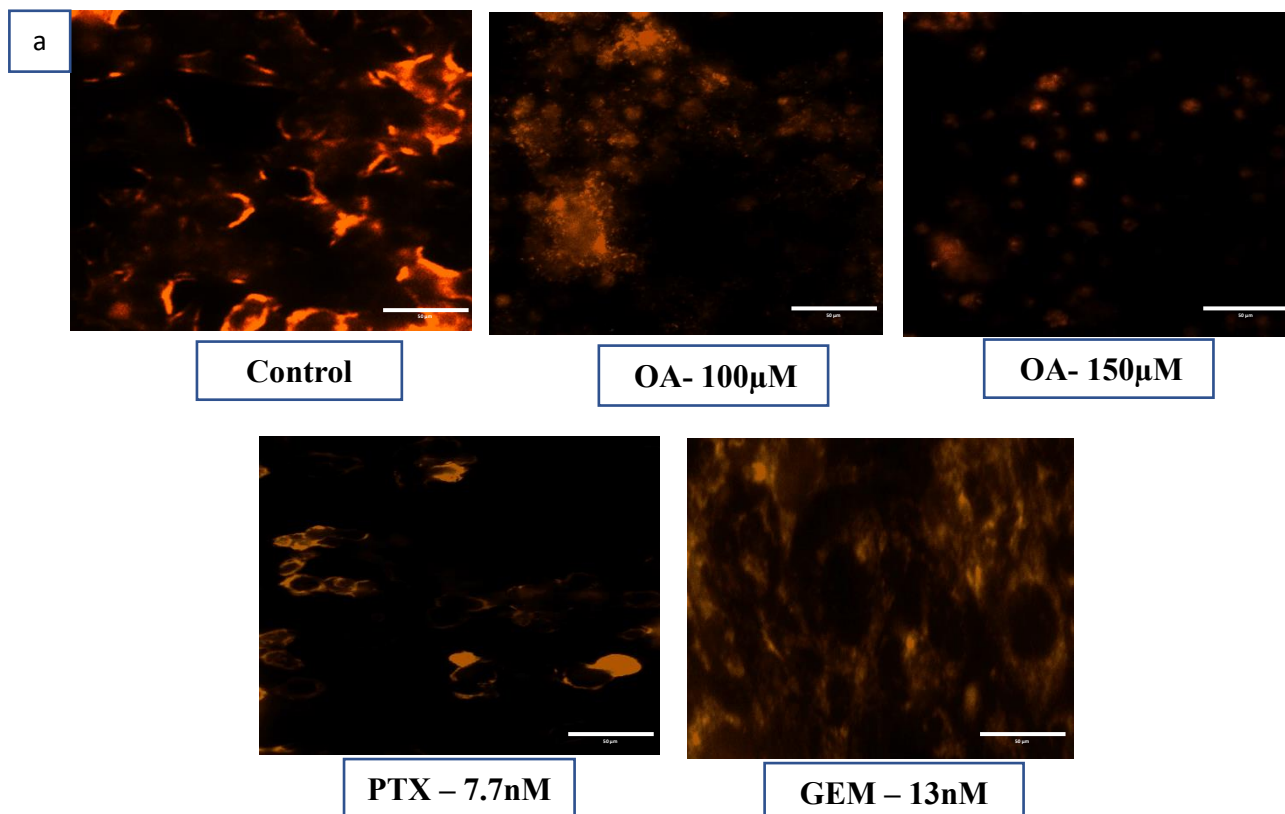
## Effect of phytochemicals from *Bauhinia variegata* L. on Lung cancer cell lines

**Figure 5.10** (a) The effect of different concentrations of PFF3, PFF4 and combination of PFF3 & PXT at 24 hr was analysed by comet assay. (b) Quantification of comet length (x 400).

### 5.3.5 Assessment of Mitochondrial membrane potential ( $\Delta\Psi_m$ )

#### 5.3.5.1 Evaluation of Mitochondrial membrane potential in A549 cells

Using tetramethylrhodamine methyl ester (TMRM), we looked into how OA treatment on A549 cells for 48 h affects  $\Delta\Psi_m$ . In proportion to  $\Delta\Psi_m$ , this red fluorescent dye builds up in mitochondria. The relationship between the mitochondrial membrane potential and TMRM fluorescence intensity is linear. A549 cells were treated with different concentrations of oleic acid for 48 h and it was observed that OA treated cells showed decrease in mitochondrial membrane potential ( $\Delta\Psi_m$ ) in A549 cells with increasing concentration of OA as compared to control cells as shown in Figure 5.11a. This may be due to disruptions in the electron transport chain and a resulting decrease in the proton motive force. Additionally, the activation of apoptotic pathways can lead to the release of cytochrome c, which can also cause a decrease in  $\Delta\Psi_m$  by releasing protons from the intermembrane space. These changes can ultimately lead to cell death.



## Effect of phytocomponents from *Bauhinia variegata* L. on Lung cancer cell lines

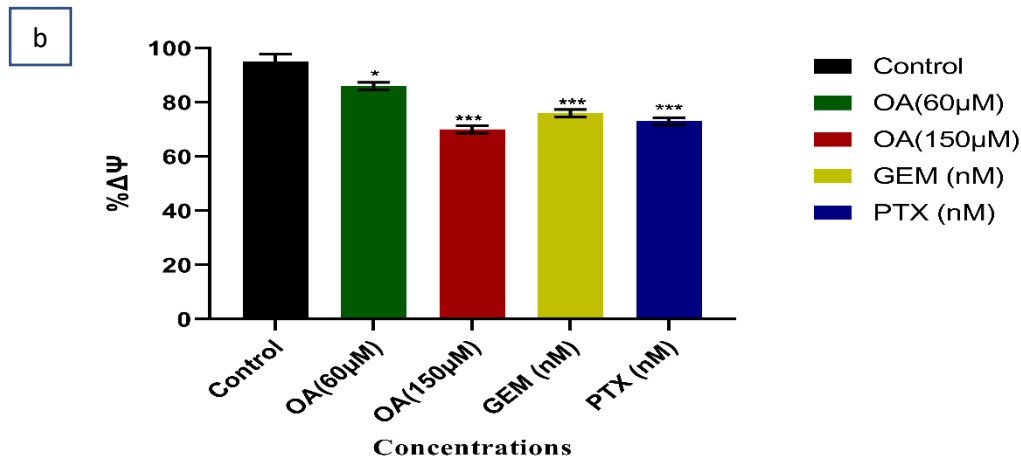
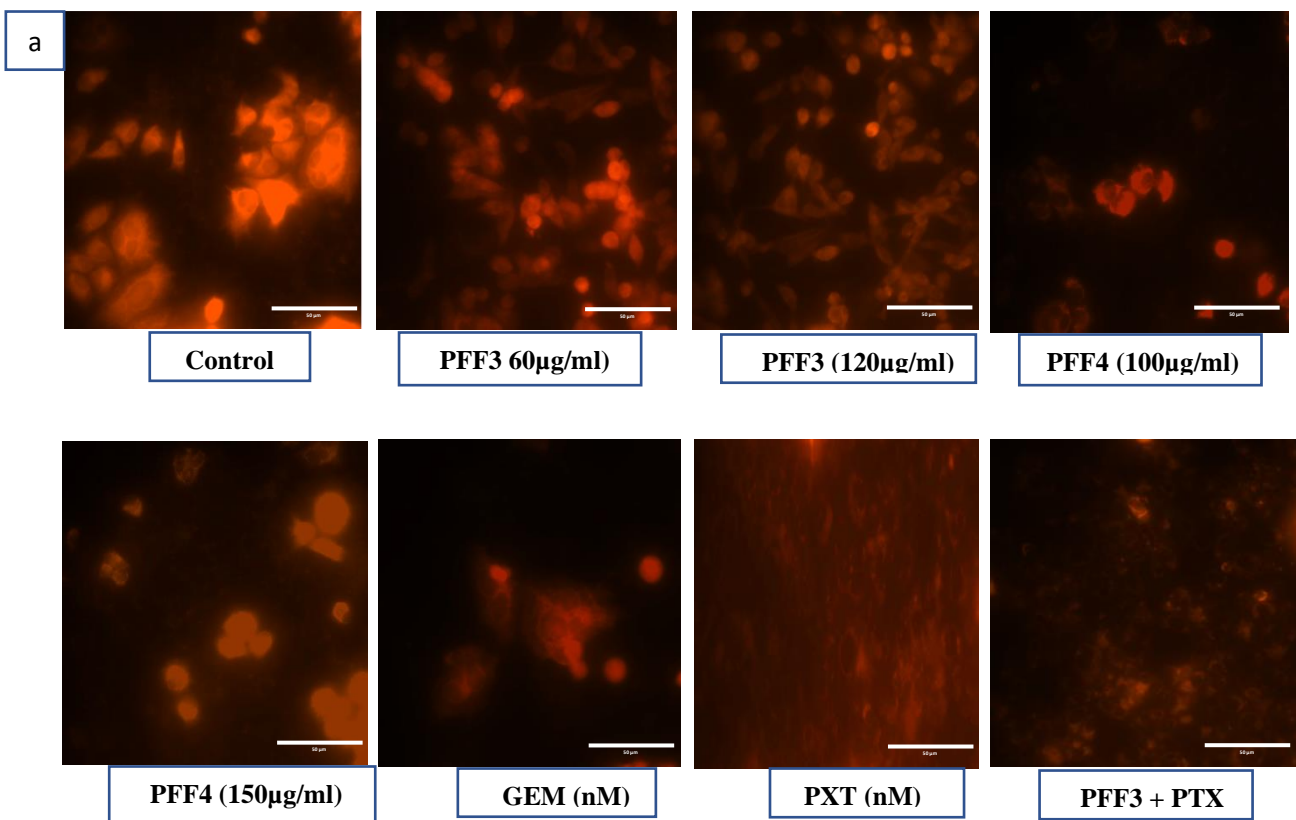


**Figure 5.11** (a) Mitochondrial membrane potential induced by treatment of OA for 48 h using fluorescent dye TMRM. (b) Quantification of fluorescent intensity (x 400). \* $p < 0.05$  is considered statistically significant.

### 5.3.5.2 Evaluation of Mitochondrial membrane potential in H460 cells

The effect of defined concentrations of PFF3, PFF4 and the combination of PFF3+PTX at (50 $\mu$ g/ml +1.75nM) for 24 hr was observed. Treatment with defined concentrations of PFF3, PFF4 results in a decrease in mitochondrial membrane potential ( $\Delta\Psi_m$ ) in NCI-H460 cells through multiple mechanisms as shown in Figure 5.12 a. The combination of PFF3+PTX at (50 $\mu$ g/ml +1.75nM) showed more decrease in  $\Delta\Psi_m$  as compared to control cells. This reduction in  $\Delta\Psi_m$  can ultimately impair mitochondrial function and trigger cell death in these cells. Paclitaxel and gemcitabine also induced decrease in mitochondrial membrane potential as compared to control cells.



## Effect of phytochemicals from *Bauhinia variegata* L. on Lung cancer cell lines

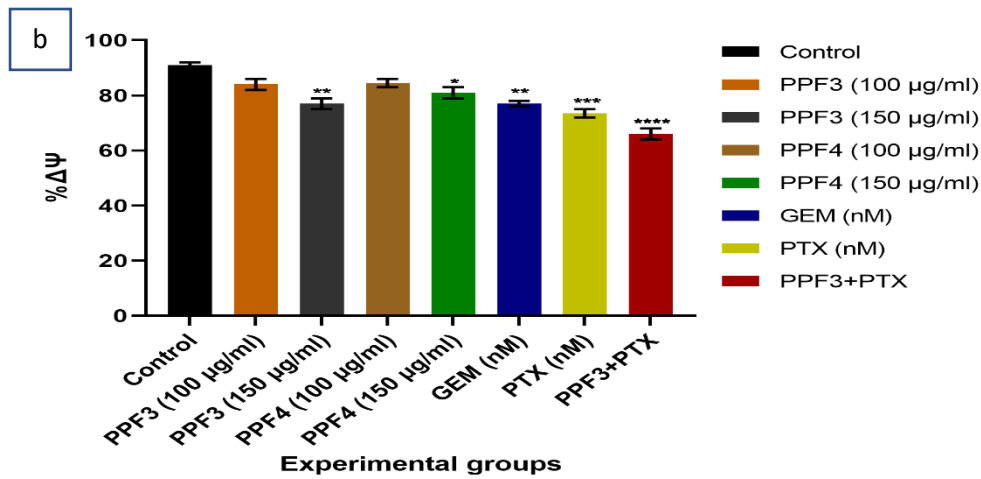
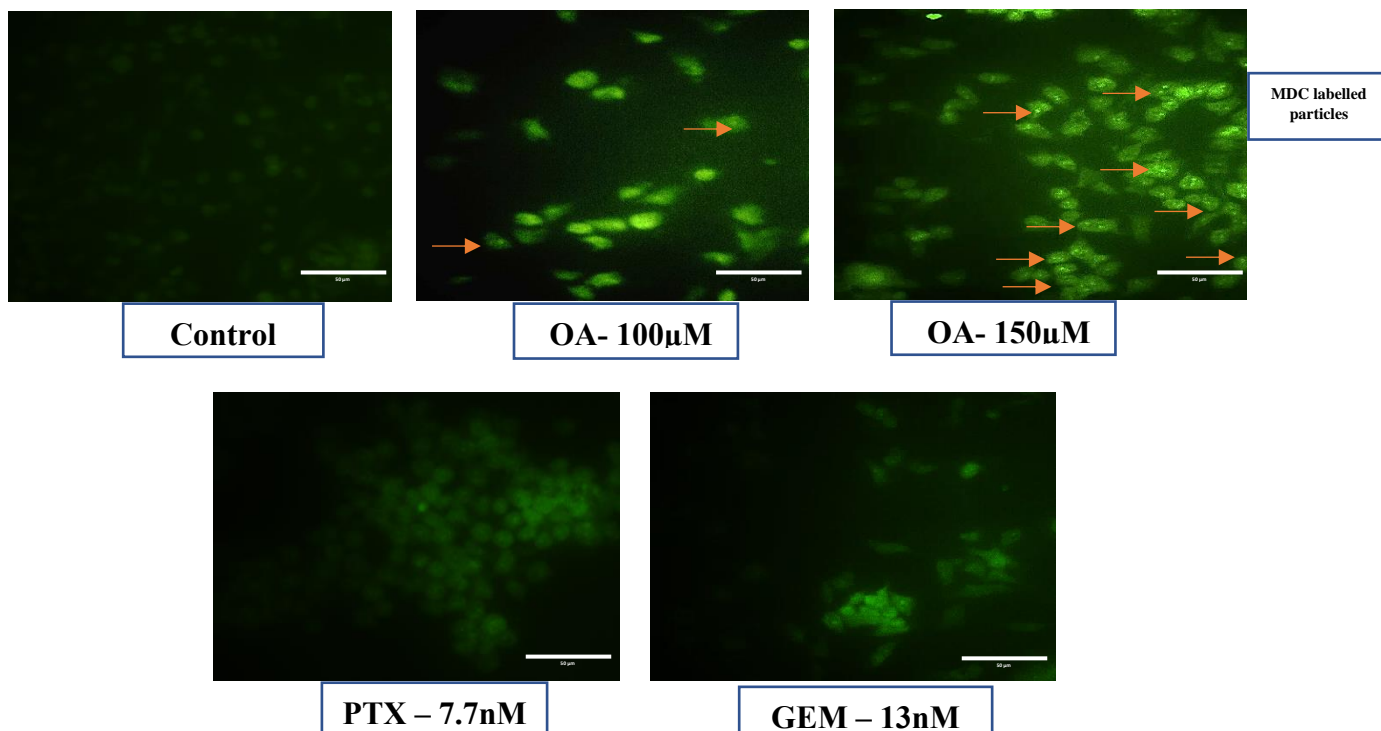


**Figure 5.12** (a) Mitochondrial membrane potential induced by treatment of different concentrations of PPF3, PPF4 and combination treatment for 24 h using fluorescent dye TMRM. (b) Quantification of fluorescent intensity (x 400). \* $p < 0.05$  is considered statistically significant.

### 5.3.6 MDC staining to detect acidic vesicular organelles (A549 cells)

Under stress conditions, lysosomes degrade cytoplasmic components through a process called autophagy. MDC is used as a marker of autophagy to detect autophagy in A549 cells. A549 cells were treated with different concentrations of OA for 48 hr and observed under fluorescence microscope. As shown in Figure 5.13, OA at 150  $\mu\text{M}$  concentration, induced the accumulation of MDC-labelled particles in A549 cells in comparison to OA lower concentration. Small number and size of MDC-labelled particles reflects low basal level of autophagy in cells.



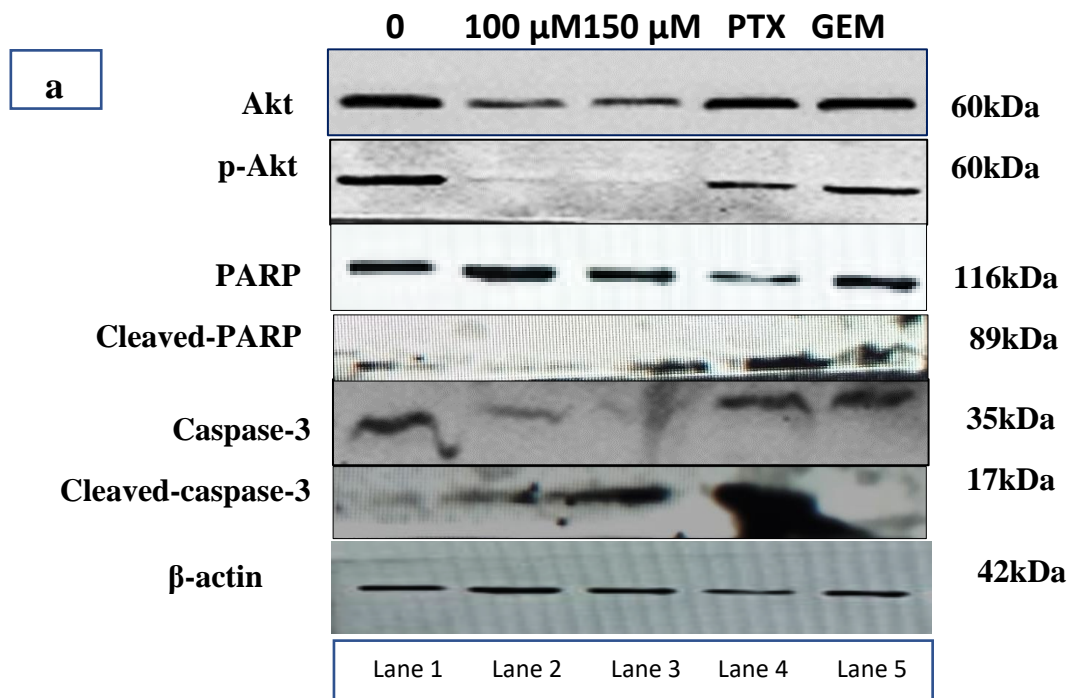
## Effect of phytocomponents from *Bauhinia variegata* L. on Lung cancer cell lines

**Figure 5.13** A549 cells were treated with different concentrations of OA to detect autophagy by MDC staining. (x 400).

### 5.3.7 Immunoblotting analysis

#### 5.3.7.1 Oleic acid inhibits anti-apoptosis and induces pro-apoptosis in A549 cells

To understand the mechanism associated with cell death caused by Oleic acid in A549 cells, western blot analysis was done to determine the relative levels of proteins associated with apoptosis in A549 cells. A549 cells were treated with Oleic acid as well as with Paclitaxel (7.7nM) and Gemcitabine (13nM) for 48 hr and expression levels of different proteins were determined as shown in Figure 5.14a. The data showed that the increasing concentration of Oleic acid induced a decrease in p-Akt expressions as compared to standards (PXT & Gem) (Figure 5.14a). In comparison to control cells and standards, decrease in Akt levels were also observed which could be due to increase in Akt protein degradation. Further, expression levels of PARP and caspase-3 showed increased expression levels of cleaved PARP and cleaved caspase-3 (at 150  $\mu$ M). Thus it can be concluded that Oleic acid treatment for 48 h showed remarkable activity in A549 cells.



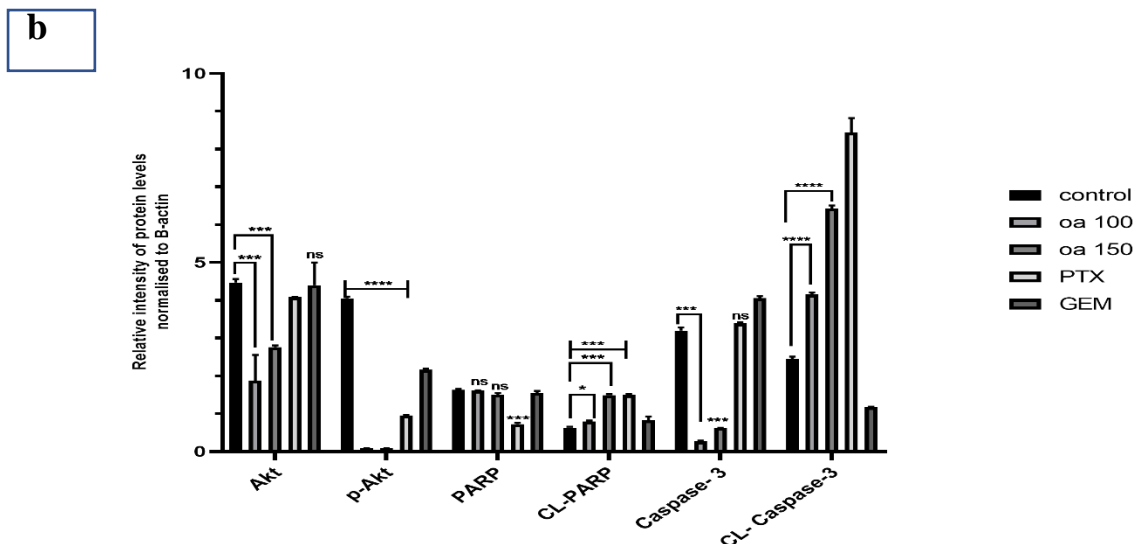


**Figure 5.14 (a)** Effect of Oleic acid on expression levels of apoptotic proteins in A549 cells by western blot analysis.  $\beta$ -actin was used as a loading control. (b) Densitometric analysis analyzed by Image J software (n=3).

### 5.3.7.2 PFF3 and PFF4 effect on expression levels of apoptotic proteins in H460 cells

Western blot analysis to determine expression of apoptotic proteins was done for H460 cells. The expression levels of PARP and Caspase-9 is shown below in H460 cells. But due to unavailability of antibodies, further experiments could not be performed on H460 cells.

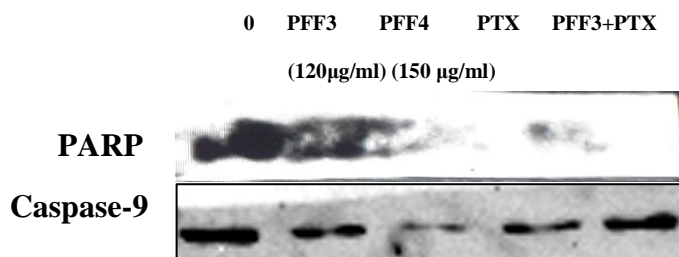


**Figure 5.15** Effect of PFF3, PFF4 and combination treatment on expression levels of apoptotic proteins in H460 cells by western blot analysis.

## 5.4 Conclusion

The study investigated the effects of Oleic acid on A549 cells and PFF3 and PFF4 as well as the combination of PFF3 & PTX on H460 cells using scratch assays and by assaying different parameters involved in cell death. Oleic acid treatment resulted in reduced cell migration and

## Effect of phytochemicals from *Bauhinia variegata* L. on Lung cancer cell lines

increased ROS levels in A549 cells. PFF3 and PFF4 treatment reduced H460 cell migration and induced ROS generation, while the combination of PFF3 and Paclitaxel (PXT) also induced more ROS levels in H460 cells. Increase in ROS levels caused morphological changes associated with apoptosis like chromatin condensation, nuclear fragmentation, and nucleus margination. Oleic acid and PFF3 and PFF4 induced DNA damage in both A549 and H460 cell lines respectively. The combination of PFF3 and PXT at defined concentration resulted in chromosomal DNA fragmentation and apoptotic cell death. The study also observed a decrease in mitochondrial membrane potential in A549 cells and autophagy in A549 cells treated with higher concentrations of oleic acid. Previous studies have reported that the PI3K/AKT signaling pathway plays an important role in cell proliferation and survival through downstream signal transduction cascades in A549 cells. To determine whether OA has an impact on the PI3K/AKT pathway, expression levels of key proteins of this pathway following OA treatment in A549 cells were monitored. Akt protein is known to promote cell survival by inhibiting apoptotic pathways. However, in the current study, treatment of A549 cells with oleic acid led to a decrease in Akt expression and phosphorylation. This decrease in Akt activity resulted in the activation of caspase-3, which is a key player in the apoptotic pathway. Activated caspase-3 then cleaved PARP, which is a DNA repair protein, resulting in its inactivation and ultimately leading to cell death by apoptosis. This study proposes that the mechanism by which Akt expression and phosphorylation stop and cause caspase-3 activation, PARP cleavage in A549 cells involves a decrease in Akt activity, which allows caspase-3 to be activated and subsequently cleave PARP, leading to cell death. However, the molecular mechanism associated with cell death in H460 cells, need to explored.

### 5.5 References

1. Lambert AW, Pattabiraman DR, Weinberg RA. Emerging Biological Principles of Metastasis. *Cell*. 2017;168(4):670-691. doi:10.1016/j.cell.2016.11.037
2. Millar FR, Janes SM, Giangreco A. Epithelial cell migration as a potential therapeutic target in early lung cancer. *Eur Respir Rev*. 2017;26(143):1-6. doi:10.1183/16000617.0069-2016
3. Mak M, Spill F, Kamm RD, Zaman MH. Single-cell migration in complex microenvironments: Mechanics and signaling dynamics. *J Biomech Eng*. 2016;138(2):1-8. doi:10.1115/1.4032188

## Effect of phytochemicals from *Bauhinia variegata* L. on Lung cancer cell lines

4. Zacharias M, Brcic L, Eidenhammer S, Popper H. Bulk tumour cell migration in lung carcinomas might be more common than epithelial-mesenchymal transition and be differently regulated. *BMC Cancer*. 2018;18(1):1-13. doi:10.1186/s12885-018-4640-y
5. Raudenská M, Petrláková K, Juriňáková T, et al. Engine shutdown: migrastatic strategies and prevention of metastases. *Trends in Cancer*. 2023;9(4):293-308. doi:10.1016/j.trecan.2023.01.001
6. Han T, Kang D, Ji D, et al. How does cancer cell metabolism affect tumor migration and invasion? *Cell Adhes Migr*. 2013;7(5):395-403. doi:10.4161/cam.26345
7. Arfin S, Jha NK, Jha SK, et al. Oxidative stress in cancer cell metabolism. *Antioxidants*. 2021;10(5):1-28. doi:10.3390/antiox10050642
8. Pistritto G, Trisciuglio D, Ceci C, Alessia Garufi, D'Orazi G. Apoptosis as anticancer mechanism: Function and dysfunction of its modulators and targeted therapeutic strategies. *Aging (Albany NY)*. 2016;8(4):603-619. doi:10.18632/aging.100934
9. Peng F, Liao M, Qin R, et al. Regulated cell death (RCD) in cancer: key pathways and targeted therapies. *Signal Transduct Target Ther*. 2022;7(1). doi:10.1038/s41392-022-01110-y
10. Liu G, Pei F, Yang F, et al. Role of autophagy and apoptosis in non-small-cell lung cancer. *Int J Mol Sci*. 2017;18(2). doi:10.3390/ijms18020367
11. MacKenzie SH, Clark AC. Targeting cell death in tumors by activating caspases. *Curr Cancer Drug Targets*. 2008;8(2):98-109. <http://www.ncbi.nlm.nih.gov/pubmed/18336192><http://www.pubmedcentral.nih.gov/articlerender.fcgi?artid=PMC3119715>
12. Hensley P, Mishra M, Kyprianou N. Targeting caspases in cancer therapeutics. *Biol Chem*. 2013;394(7):831-843. doi:10.1515/hsz-2013-0128
13. Mandelkow R, Gümbel D, Ahrend H, et al. Detection and Quantification of Nuclear Morphology Changes in Apoptotic Cells by Fluorescence Microscopy and Subsequent Analysis of Visualized Fluorescent Signals. 2017;2244:2239-2244. doi:10.21873/anticancerres.11560
14. Duddukuri NK, Thatikonda S, Godugu C, Kumar RA, Doijad N. Synthesis of Novel Thiophene-Chalcone Derivatives as Anticancer- and Apoptosis-Inducing Agents.

## Effect of phytochemicals from *Bauhinia variegata* L. on Lung cancer cell lines

- ChemistrySelect*. 2018;3(24):6859-6864. doi:10.1002/slct.201800613
15. Azqueta A, Slysikova J, Langie SAS, Gaivão ION, Collins A. Comet assay to measure DNA repair : approach and applications. 2014;5(August):1-8. doi:10.3389/fgene.2014.00288
  16. Liao W, Mcnutt MA, Zhu W. The comet assay : A sensitive method for detecting DNA damage in individual cells. *Methods*. 2009;48(1):46-53. doi:10.1016/j.ymeth.2009.02.016
  17. Aggarwal V, Tuli HS, Varol A, et al. Role of reactive oxygen species in cancer progression: Molecular mechanisms and recent advancements. *Biomolecules*. 2019;9(11). doi:10.3390/biom9110735
  18. Nakamura H, Takada K. Reactive oxygen species in cancer: Current findings and future directions. *Cancer Sci*. 2021;112(10):3945-3952. doi:10.1111/cas.15068
  19. Choi I. Reactive Oxygen Species and Cancer. *Hanyang Med Rev*. 2013;33(2):118. doi:10.7599/hmr.2013.33.2.118
  20. Zaidieh T, Smith JR, Ball KE, An Q. ROS as a novel indicator to predict anticancer drug efficacy. *BMC Cancer*. 2019;19(1):1-14. doi:10.1186/s12885-019-6438-y
  21. Murugan S, Amaravadi RK. HHS Public Access. 2017;1:145-166. doi:10.1007/978-3-319-26666-4
  22. Wang R, Zhang Q, Peng X, et al. Stelletin B Induces G1 Arrest , Apoptosis and Autophagy in Human Non-small Cell Lung Cancer A549 Cells via Blocking PI3K / Akt / mTOR Pathway. *Nat Publ Gr*. 2016;(May):1-10. doi:10.1038/srep27071
  23. Seervi M, Rani A, Sharma AK, Kumar TRS. Biomedicine & Pharmacotherapy ROS mediated ER stress induces Bax-Bak dependent and independent apoptosis in response to Thioridazine. *Biomed Pharmacother*. 2018;106(June):200-209. doi:10.1016/j.biopha.2018.06.123
  24. Liebmann JE, Cook JA, Lipschultz C, Teague D, Fisher J, Mitchell JB. Cytotoxic studies of paclitaxel (Taxol®) in human tumour cell lines. *Br J Cancer*. 1993;68(6):1104-1109. doi:10.1038/bjc.1993.488
  25. Lin W, Ye H. Anticancer activity of ursolic acid on human ovarian cancer cells via ROS

## Effect of phytochemicals from *Bauhinia variegata* L. on Lung cancer cell lines

and MMP mediated apoptosis, cell cycle arrest and downregulation of PI3K/AKT pathway. *J BUON*. 2020;25(2):750-756.

26. Balaji S, Mohamed Subarkhan MK, Ramesh R, Wang H, Semeril D. Synthesis and Structure of Arene Ru(II) NAO-Chelating Complexes: In Vitro Cytotoxicity and Cancer Cell Death Mechanism. *Organometallics*. 2020;39(8):1366-1375. doi:10.1021/acs.organomet.0c00092
27. Olive PL, Banáth JP. The comet assay: a method to measure DNA damage in individual cells. *Nat Protoc*. 2006;1(1):23-9. doi: 10.1038/nprot.2006.5. PMID: 17406208.
28. Toriyama, K., Okuma, T., Abe, S., Nakamura, H., & Aoshiba, K. (2024). In vitro anticancer effect of azithromycin targeting hypoxic lung cancer cells via the inhibition of mitophagy. *Oncology Letters*, 27, 12. <https://doi.org/10.3892/ol.2023.14146>